Article

TRANSPARENT PROCESS

EMBO reports

H3K14 ubiquitylation promotes H3K9 methylation for heterochromatin assembly

Eriko Oya[1,2,†], Reiko Nakagawa[3], Yuriko Yoshimura[4], Mayo Tanaka[4], Gohei Nishibuchi[1,‡], Shinichi Machida[5,§], Atsuko Shirai[6], Karl Ekwall[2], Hitoshi Kurumizaka[5,7], Hideaki Tagami[1] & Jun-ichi Nakayama[1,4,8,*]

Abstract

The methylation of histone H3 at lysine 9 (H3K9me), performed by the methyltransferase Clr4/SUV39H, is a key event in heterochromatin assembly. In fission yeast, Clr4, together with the ubiquitin E3 ligase Cul4, forms the Clr4 methyltransferase complex (CLRC), whose physiological targets and biological role are currently unclear. Here, we show that CLRC-dependent H3 ubiquitylation regulates Clr4's methyltransferase activity. Affinity-purified CLRC ubiquitylates histone H3, and mass spectrometric and mutation analyses reveal that H3 lysine 14 (H3K14) is the preferred target of the complex. Chromatin immunoprecipitation analysis shows that H3K14 ubiquitylation (H3K14ub) is closely associated with H3K9me-enriched chromatin. Notably, the CLRC-mediated H3 ubiquitylation promotes H3K9me by Clr4, suggesting that H3 ubiquitylation is intimately linked to the establishment and/or maintenance of H3K9me. These findings demonstrate a cross-talk mechanism between histone ubiquitylation and methylation that is involved in heterochromatin assembly.

Keywords epigenetic gene silencing; fission yeast; heterochromatin; histone methylation; histone ubiquitylation

Subject Category Chromatin, Transcription & Genomics

DOI 10.15252/embr.201948111 | Received 17 March 2019 | Revised 7 August 2019 | Accepted 9 August 2019 | Published online 29 August 2019

EMBO Reports (2019) 20: e48111

Introduction

In eukaryotic cells, the formation of higher-order chromatin structure, known as heterochromatin, plays an important role in diverse chromosomal processes. Heterochromatin assembly is intimately associated with changes in post-translational histone-tail modifications [1–3]. Histone H3 lysine 9 methylation (H3K9me), a hallmark of heterochromatin structure, is catalyzed by SUV39H-family histone methyltransferases (HMTases) and functions as a binding site for recruiting heterochromatin protein 1 (HP1) family proteins [4–6]. Heterochromatic structures are epigenetically inherited through cell division in a metastable manner [7,8].

In the fission yeast *Schizosaccharomyces pombe* (*S. pombe*), heterochromatin plays critical roles in the assembly of functional chromosomal domains such as centromeres, telomeres, and the mating-type loci [3,9]. Clr4, a homolog of mammalian SUV39H, is the sole H3K9 methyltransferase expressed in *S. pombe* and plays a central role in heterochromatin assembly [4,6,10]. H3K9me creates binding sites for the chromodomain (CD) proteins Swi6, Chp1, and Chp2, and these proteins further recruit a variety of chromatin proteins to form repressive higher-order chromatin [11–14]. Clr4 also possesses a CD that can bind H3K9me, and it has been suggested that the ability of Clr4 and other HMTases to "write" and "read" H3K9me facilitates heterochromatin spreading and the maintenance of H3K9me during cell division [15].

In fission yeast, the assembly and maintenance of pericentromeric heterochromatin is directly linked to the RNA interference (RNAi) pathway [3,16–18]. Pericentromeric repeats are transcribed by RNA polymerase II, and the nascent RNAs are converted to small interfering RNAs (siRNAs) through the actions of the RNA-dependent RNA polymerase complex (RDRC) and Dicer (Dcr1) ribonuclease. The siRNAs are then loaded onto Argonaute (Ago1), the catalytic component of the RNA-induced transcriptional silencing (RITS) complex, which targets pericentromeric repeats through base-pairing interaction between the

1 Graduate School of Natural Sciences, Nagoya City University, Nagoya, Japan
2 Department of Biosciences and Nutrition, Karolinska Institutet, Huddinge, Sweden
3 Laboratory for Phyloinformatics, RIKEN Center for Biosystems Dynamics Research, Kobe, Japan
4 Division of Chromatin Regulation, National Institute for Basic Biology, Okazaki, Japan
5 Laboratory of Structural Biology, Graduate School of Advanced Science and Engineering, Waseda University, Shinjuku-ku, Tokyo, Japan
6 Cellular Memory Laboratory, RIKEN, Wako, Japan
7 Laboratory of Chromatin Structure and Function, Institute for Quantitative Biosciences, The University of Tokyo, Bunkyo-ku, Tokyo, Japan
8 Department of Basic Biology, School of Life Science, The Graduate University for Advanced Studies (SOKENDAI), Okazaki, Japan
*Corresponding author. Tel: +81 564 55 7680; E-mail: jnakayam@nibb.ac.jp
†Present address: Faculty of Science and Engineering, Chuo University, Bunkyo-ku, Tokyo, Japan
‡Present address: Graduate School of Science, Osaka University, Toyonaka, Japan
§Present address: Institute of Human Genetics, CNRS UMR 9002, Montpellier, France

siRNAs and nascent transcripts. In addition to Ago1, the RITS complex contains the GW motif protein Tas3 and the chromodomain protein Chp1, and the association of the RITS complex with chromatin is facilitated by the Chp1-CD's H3K9me-binding and nucleic acid-binding activities [19]. The deletion of RNAi pathway components leads to a loss of silencing and reduced H3K9me at the pericentromeric regions, indicating that the RNAi pathway and recruitment of the siRNA-bound RITS complex to chromatin are coupled with the targeting of Clr4. While RNAi also targets the silent mating-type loci and telomeres, alternative pathways act redundantly with the RNAi pathway to recruit the Clr4 HMTase activity [20,21].

Clr4 forms a multi-protein complex called the Clr4 methyltransferase complex (CLRC). The CLRC consists of the cullin scaffold protein Cul4, the β-propeller protein Rik1, the WD-40 protein Raf1 (Dos1/Cmc1/Clr8), the replication foci targeting sequence (RFTS)-like domain-containing protein Raf2 (Dos2/Cmc2/Clr7), and the RING-box protein Rbx1 (Pip1) [22–26]. All of these CLRC components except Rbx1 have been shown to be required for heterochromatic silencing. Cul4, Rik1, and Raf1 in fission yeast show a strong structural resemblance to the conserved CUL4-DDB1-DDB2 E3 ubiquitin ligase ($CRL4^{DDB1}$) [27,28]. While Raf2 has no analogous component in the $CRL4^{DDB1}$ complex, it interacts with Cul4, Rik1, and Raf1, and thus is proposed to be a hub for the core components in the CLRC [28,29]. Deleting genes encoding CLRC components results in the loss of both H3K9 methylation and siRNA [24,30], indicating that a physical interaction between CLRC and RITS couples the siRNA production with H3K9 methylation. Stc1, a tandem zinc finger domain-containing protein, was not identified among the CLRC components, but was shown to mediate the interaction between the CLRC and RITS, presumably through interactions with Raf2 and Ago1 [31,32]. On the other hand, studies using *cul4* mutant cells suggested that Rik1 is loaded onto heterochromatic repeats in an RNAi-dependent manner and targets other CLRC components to heterochromatic loci [15,25]. Intriguingly, analyses of cells expressing mutant histone H3 (H3K9R) or CLRC components demonstrated that the CLRC complex promotes siRNA production, independently of H3K9 methylation [27,29,33], although the details of the mechanism remain unknown.

As predicted from its structural similarity to $CRL4^{DDB1}$, the CLRC exhibits ubiquitin ligase activity *in vitro* [22]. In addition, heterochromatin defects in Cul4 mutants cannot be rescued by expressing a Cul4 protein lacking Nedd8 modification, which is essential for its ubiquitin ligase activity [25,34]. These data show that the CLRC is an active ubiquitin ligase whose ligase activity is required for heterochromatin formation. Structural and functional studies also suggested that Raf1 plays a critical role in target recognition by the CLRC [27,28]. However, whether the CLRC acts as an E3 ubiquitin ligase *in vivo* and how ubiquitylation modulates Clr4's HMTase activity remain unclear.

Here, we demonstrated that affinity-purified CLRC preferentially ubiquitylates lysine 14 on histone H3 (H3K14) *in vitro*, and the H3K14 ubiquitylation is tightly associated with H3K9me-enriched heterochromatin *in vivo*. Importantly, the K14-ubiquitylated H3 promotes H3K9's methylation by Clr4. This study demonstrates a cross-talk mechanism between histone methylation and ubiquitylation for heterochromatin assembly.

Results

Histone H3 is ubiquitylated *in vitro* by the CLRC

To identify the physiological substrate(s) ubiquitylated by CLRC, we first affinity-purified the CLRC and characterized it. For this purpose, an *S. pombe* strain expressing C-terminally TAP-tagged Rik1 (Rik1-TAP) was constructed, and Rik1-TAP and its associated proteins were affinity-purified. Analysis of the purified fraction revealed protein bands that were specific to the Rik1-TAP preparation but were absent from a control preparation using an untagged strain (mock) (Fig 1A). Mass spectrometry analysis of the purified fraction identified a number of specific proteins, including Cul4, Nedd8, Raf2, Raf1, and Clr4, in agreement with previous studies (Fig 1A) [22,24,25,27]. In addition, a limited number of histone H2B or H4 peptides were detected in the purified fraction, as previously observed [22,24]. Rik1 is reported to form a protein complex with Mms19 and Cdc20 [35], but these two proteins were not identified in our Rik1-TAP preparations.

Given that histones have been identified in several independent Rik1-TAP purifications [22,24] and that histone ubiquitylation has a direct effect on other histone-modifying enzymes [36,37], we chose histones as candidate CLRC substrates and examined whether CLRC ubiquitylates them. We performed an *in vitro* ubiquitylation assay using recombinant E1, E2 (UbcH5b), biotinylated ubiquitin, and histones. Incubation of the Rik1-TAP preparation with these components in the absence of histone substrate resulted in a ladder of biotinylated ubiquitin (Fig 1B, lane 3, and Fig EV1A–C). The ladder probably represented the self-ligation of polyubiquitin in the absence of substrate [38,39], and its appearance suggested that the purified CLRC possessed ubiquitin ligase activity. When histone H3 was added as a substrate, several additional bands appeared, whose molecular weights corresponded to histone H3 modified with mono (~8.6 kDa)- or di-ubiquitin (~17 kDa) (Fig 1B, lane 4, indicated by asterisks). This activity appeared to be specific for the Rik1-TAP preparation, since we did not detect it in the control assay using a mock preparation obtained from the Rik1-untagged strain (Fig 1B, lane 5, mock). Although a weak band (~25 kDa) was also detected in the control assay without E3 (Fig 1B, lane 2), it migrated slightly more slowly than the H3 species modified with mono-ubiquitin, and appeared to be a background product. When histone H2A, H2B, or H4 was used in the assay, a very weak activity was detected for H2A (Fig EV1A, indicated by asterisks), and no obvious change was seen for H2B or H4 (Fig EV1B and C). Although H2A might also serve as a substrate of CLRC, the purified CLRC exhibited a stronger activity for H3, and thus, in this study, we focused on H3's ubiquitylation and its roles in heterochromatin assembly.

Characterization of CLRC's H3 ubiquitylation activity

Cul4 functions as scaffold to form E3 ubiquitin ligase and is modified by the ubiquitin-like protein Nedd8, which induces the E3 ubiquitin ligase activity [34]. To determine whether Cul4's activity is involved in the CLRC's H3 ubiquitylation, we first created a *cul4* mutant allele in which Lys680 (the site of Nedd8 conjugation) was mutated to arginine ($cul4^{K680R}$) as previously reported [25].

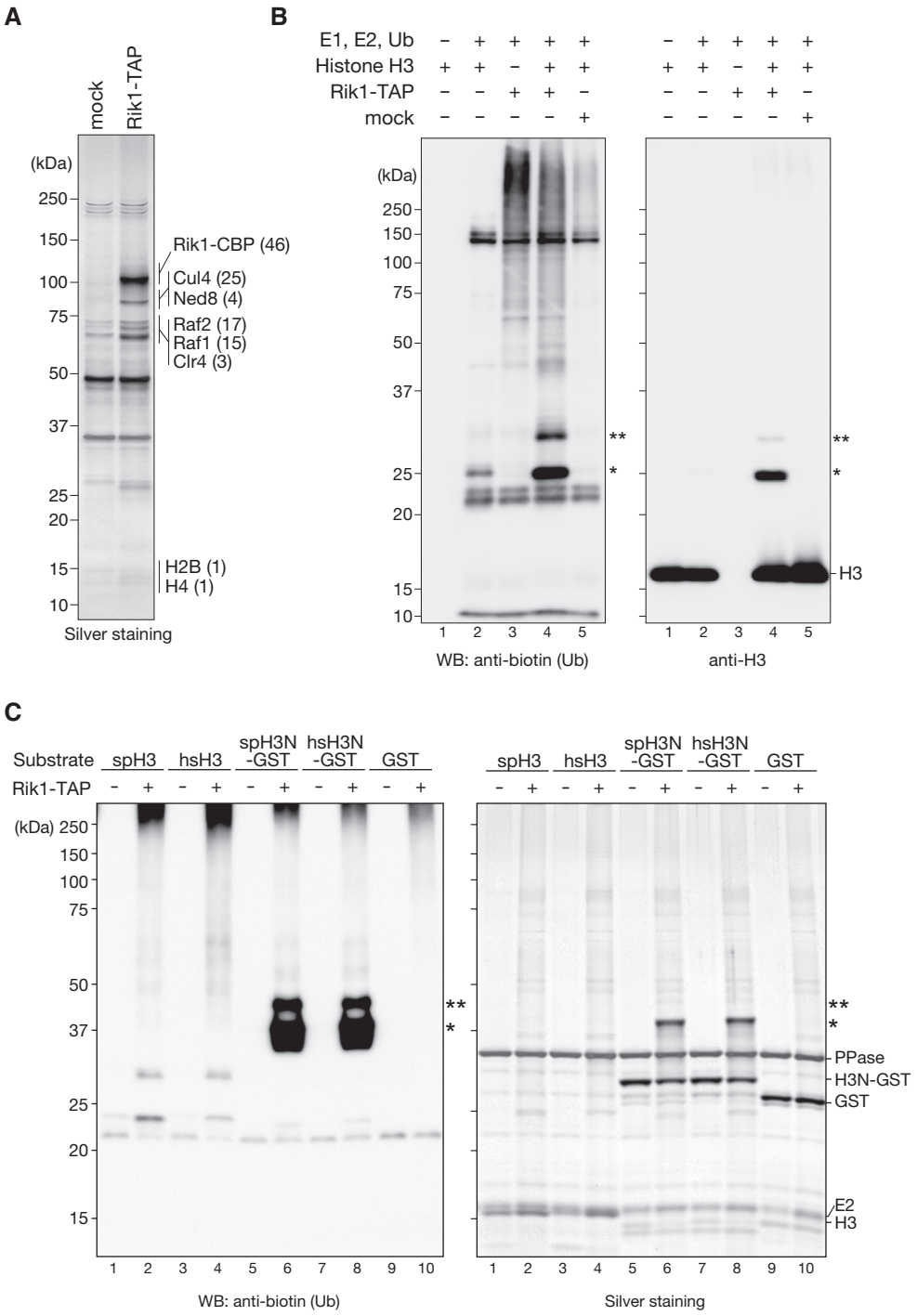

Figure 1. Histone H3 is ubiquitylated *in vitro* by the CLRC.

A Purified TAP-tagged Rik1-containing complexes analyzed by SDS–PAGE and silver staining. mock: a mock purification from an untagged strain. Proteins identified by LC-MS/MS are indicated at right, with the number of identified unique peptides in parentheses.

B *In vitro* ubiquitylation assays using biotinylated ubiquitin, purified CLRC, and recombinant *S. pombe* histone H3 as the substrate. Proteins were analyzed by Western blotting (WB) using the indicated antibodies. Asterisks indicate ubiquitylated histone H3 species.

C Ubiquitylation assays using recombinant histone H3, the N-terminal tail of histone H3 (residues 1-36) fused with GST (H3N-GST), or GST alone as the substrate. Both fission yeast (sp) and human (hs) full-length H3 proteins and H3N-GST fusion proteins were examined. The proteins were analyzed by SDS–PAGE followed by either silver staining or Western blotting with an anti-biotin antibody. Asterisks indicate ubiquitylated histone H3 species.

However, the *cul4* ^{K680R} mutant showed a severe growth defect (Fig EV2B), which made it difficult to assess Cul4's involvement in CLRC's H3 ubiquitylation. Instead, we isolated a milder *cul4* mutant allele (*cul4-1*), which did not exhibit a noticeable growth defect (Fig EV2B), but resulted in loss of the silencing of *ade6*$^+$ or *ura4*$^+$ marker genes inserted at the centromeric repeats (*otr1R::ade6*$^+$) and the mating-type locus (*kint2::ura4*$^+$), respectively (Fig EV2A and B). In this *cul4* mutant, its original 3′-untranslated region was replaced with *TEF* terminator and a hygromycin-resistant gene without altering *cul4* coding region, which presumably led to a change in *cul4* expression or mRNA stability. This mutation changed the profile of the Rik1-TAP preparation with a clear reduction in the co-purified Cul4 (Fig EV2C) and markedly reduced the H3 ubiquitylation activity (Fig EV2D). This result suggested that Cul4 plays a critical role in CLRC's H3 ubiquitylation activity.

To characterize the CLRC's ubiquitylation activity further, we prepared a fusion protein of the N-terminal tail of H3 (residues A1-K36) and GST (H3N-GST). Since the human H3 histone-tail sequence is slightly different from that of *S. pombe*, we prepared both human and *S. pombe* H3N-GST fusion proteins, and examined them in the ubiquitylation assay. While both the human and *S. pombe* full-length H3 histones were ubiquitylated by CLRC (Fig 1C, lanes 2 and 4), the H3N-GSTs were more efficiently ubiquitylated than the full-length histones (Fig 1C, lanes 6 and 8). These results suggested that the CLRC preferentially ubiquitylates the N-terminal tail of H3 and that the C-terminal region of H3 may have an inhibitory effect on the CLRC's activity for the H3 N-terminal tail. We also noticed that CLRC did not efficiently ubiquitylate H3 in reconstituted nucleosomes (Fig EV2E and F), suggesting that nucleosomal DNA may also have an inhibitory effect on the CLRC's activity and additional factor(s) may help to promote it *in vivo*.

CLRC preferentially ubiquitylates histone H3 lysine 14

We next sought to identify the ubiquitylated lysine residues of the H3 N-terminal tail. For this investigation, we performed mass spectrometry (LC-MS/MS) analysis of the mono- and di-ubiquitylated H3N-GST species recovered from the CLRC-mediated *in vitro* ubiquitylation assay (Figs 2A and EV3A). Because trypsin cleaves the C-terminal Arg-Gly-Gly of ubiquitin, ubiquitylated lysine residues could be identified by the presence of a characteristic diGly remnant (Fig 2B) [40]. In this analysis, four residues, K14, K18, K23, and K27, were identified as candidate H3 ubiquitylation sites (Fig EV3B). The number of identified peptides containing each of the candidate ubiquitylation sites suggested that K14 and K18 are the predominant H3 ubiquitylation sites.

To confirm the results obtained by LC-MS/MS analysis, we prepared H3N-GST fusion proteins containing amino acid substitutions for each of the candidate lysine residues (K4R, K9R, K14R, K18R, K23R, K27R, and K36R) and assessed their effect on H3's ubiquitylation. In agreement with the LC-MS/MS analysis (Fig EV3B), the K14R substitution resulted in a marked reduction in the CLRC-mediated H3 ubiquitylation (Fig 2C, indicated by asterisks). Although the K18R, K23R, or K27R substitution appeared to slightly reduce the H3 ubiquitylation, the effect was much weaker than that of the K14R substitution. The other lysine substitutions (K4R, K9R, and K36R) had little or no impact on the CLRC-mediated H3 ubiquitylation (Fig 2C). We also confirmed that K14A substitution also markedly reduced the CLRC-mediated ubiquitylation of full-length histone H3 (Fig EV3C and D). These results suggested that CLRC possesses an E3 ubiquitin ligase activity that preferentially targets histone H3K14, and that K14-mono-ubiquitylated H3 is a major product of CLRC's activity. At this point, we could not distinguish whether the di-ubiquitylated H3 species contained two mono-ubiquitins at different lysine residues or one di-ubiquitin at a single lysine residue. In either case, our findings indicated that H3K14 ubiquitylation (H3K14ub) may play a role in promoting additional ubiquitylation.

Heterochromatin is enriched in H3K14ub *in vivo*

Since our *in vitro* assays suggested that the CLRC preferentially ubiquitylates histone H3K14, we next sought to assess the presence of H3K14ub *in vivo*. We speculated that H3K14ub would be concentrated at heterochromatic regions where the CLRC is predominantly localized [15]. To examine this possibility, we carried out chromatin immunoprecipitation (ChIP) assays using antibodies against heterochromatic H3K9me2 or euchromatic H3K4me2 [41], and performed LC-MS/MS analyses to identify the histone modifications associated with these regions (Figs 3 and EV3E and F, and Appendix Table S1, Appendix Figs S1–S8). We confirmed that H3K9me2 was enriched in centromeric *dg* repeats, whereas H3K4me2 was preferentially enriched in the actively transcribed *act1*$^+$ gene (Fig EV3E). Subsequent LC-MS/MS analysis revealed that K14-ubiquitylated H3 peptides were detected exclusively in the H3K9me2-associated chromatin (Figs 3B–D and EV3F). It was also notable that nearly all of the tryptic K14-ubiquitylated H3 peptides contained H3K9me2 or H3K9me3 (Fig 3C). These results demonstrated that H3K14ub is concentrated in H3K9me-associated heterochromatin, where CLRC is predominantly localized, *in vivo*. Our LC/MS/MS analysis also revealed that K56- or K79-ubiquitylated H3 peptides were preferentially concentrated in the H3K4me2-associated chromatin (Figs 3C and D, and EV3F), although their biological functions and potential involvement in transcription are unknown.

H3K14 is critical for heterochromatin assembly *in vivo*

We next asked whether H3K14 is essential for heterochromatin assembly in fission yeast. *Schizosaccharomyces pombe* encodes three copies of genes that encode histone H3 (H3.1, H3.2, and H3.3). We introduced an alanine substitution mutation at individual lysine residues within the H3.1 N-terminal tail and assessed the effect on the silencing of *kint2::ura4*$^+$ (Fig 4A). Introduction of the K9A mutation clearly abolished the *kint2::ura4*$^+$ silencing (Fig 4B), and ChIP analysis showed that the level of H3K9me2 at heterochromatic regions was reduced to half or less that of wild type (Fig 4C). Notably, the K14A or K14R mutation also led to defective silencing and decreased H3K9me2 levels, comparable to that of the K9A mutation (Figs 4B and C, and EV4A). The status of silencing defect caused by amino acid substitution for K9 or K14 was also confirmed by quantitative reverse-transcriptase PCR (RT–qPCR) (Fig EV4B and C). Alanine substitution of the other lysine residues in the H3.1 N-terminal tail had no effect on gene silencing (Fig 4B). While these

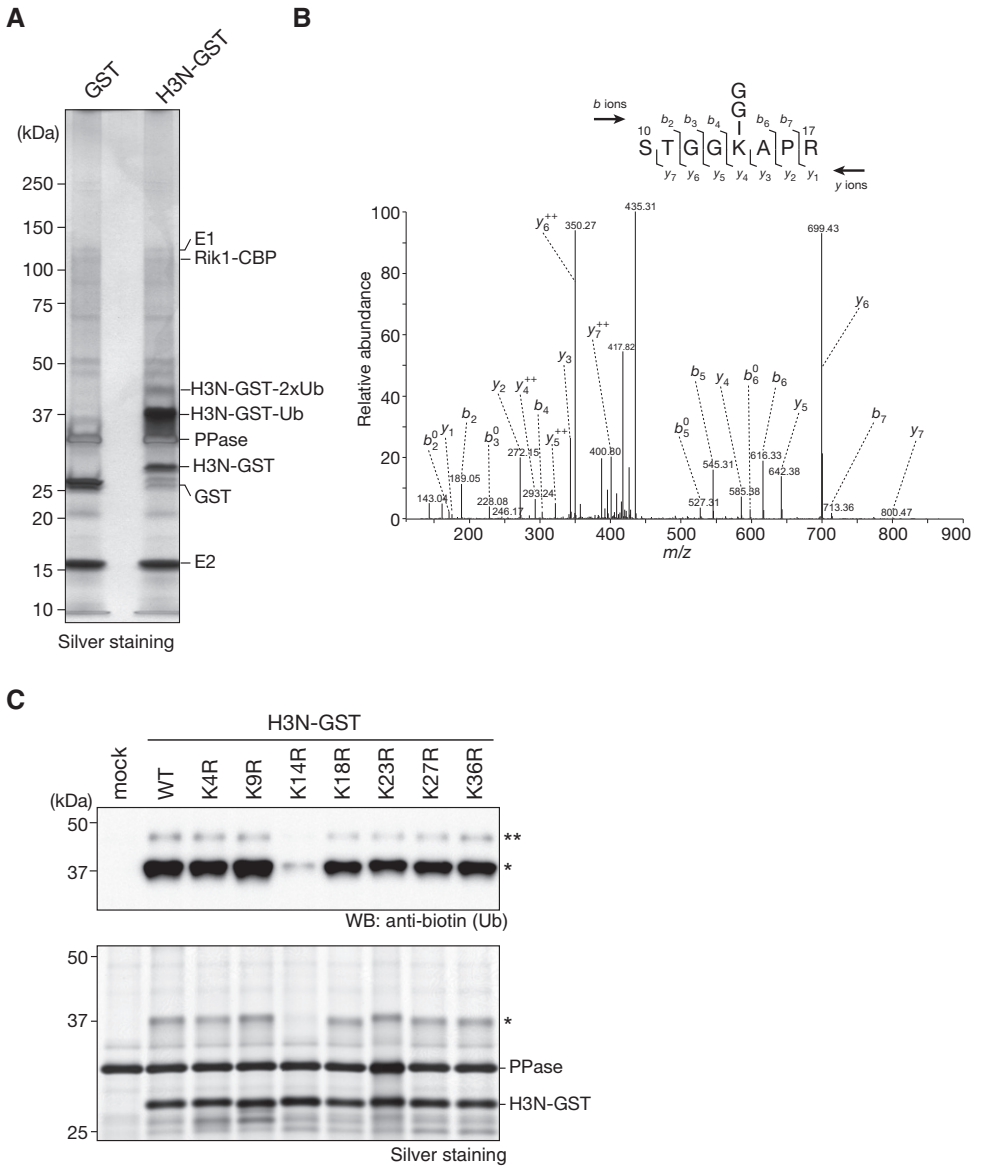

Figure 2. Histone H3 lysine 14 is ubiquitylated *in vitro* by CLRC.

A Ubiquitylation assay using H3N-GST. The components included in the assay and the ubiquitylated H3N-GST species are indicated at right.

B MS/MS spectrum of the histone H3 peptide corresponding to residues 10–17. The observed *y* and *b* ions and fragment map are shown.

C Ubiquitylation assay using biotinylated ubiquitin and recombinant wild-type H3N-GST (WT) and arginine-substituted H3N-GST mutants as substrates. Proteins were analyzed by Western blotting and silver staining. mock: reaction without substrate. Asterisks indicate ubiquitylated H3N-GST proteins.

effects were presumably due to a dominant-negative effect of the mutations in H3.1, ChIP analysis revealed that the levels of Rik1 associated with the mating-type *cenH* or centromeric *dg* locus were higher than that of wild-type cells (Fig 4D). This may imply that amino acid substitution for K9 or K14 might affect CLRC's enzymatic activity and/or inhibit its turnover at heterochromatic regions. We also noticed that these amino acid substitutions had only a limited effect on the centromeric *otr1R::ade6*$^{+}$ silencing and *dg* expression (Fig EV4D–G). As previously reported [42], clear silencing defect of *otr1R::ade6*$^{+}$ and elevated *dg* expression were observed for cells harboring single H3 gene (*hht2*) containing K9 or K14 amino acid substitution (Fig EV4F and G). The different effects on two heterochromatic regions might be attributable to the difference in pathways to promote H3K9 methylation at these regions.

To further examine the relationship between K9 and K14, we introduced combinatorial amino acid substitutions in the H3.1 N-terminal tail (Fig 4E). No additive effect was observed for cells expressing mutant H3.1 with both the K9A and K14A substitutions (Fig 4E, K9, 14A), suggesting that the silencing defect caused by K9A or K14A substitution was brought about through the same pathway. Although the K4A mutation showed a suppressing effect on K14A (Fig 4E, K4, 14A), a similar effect was seen for K9A

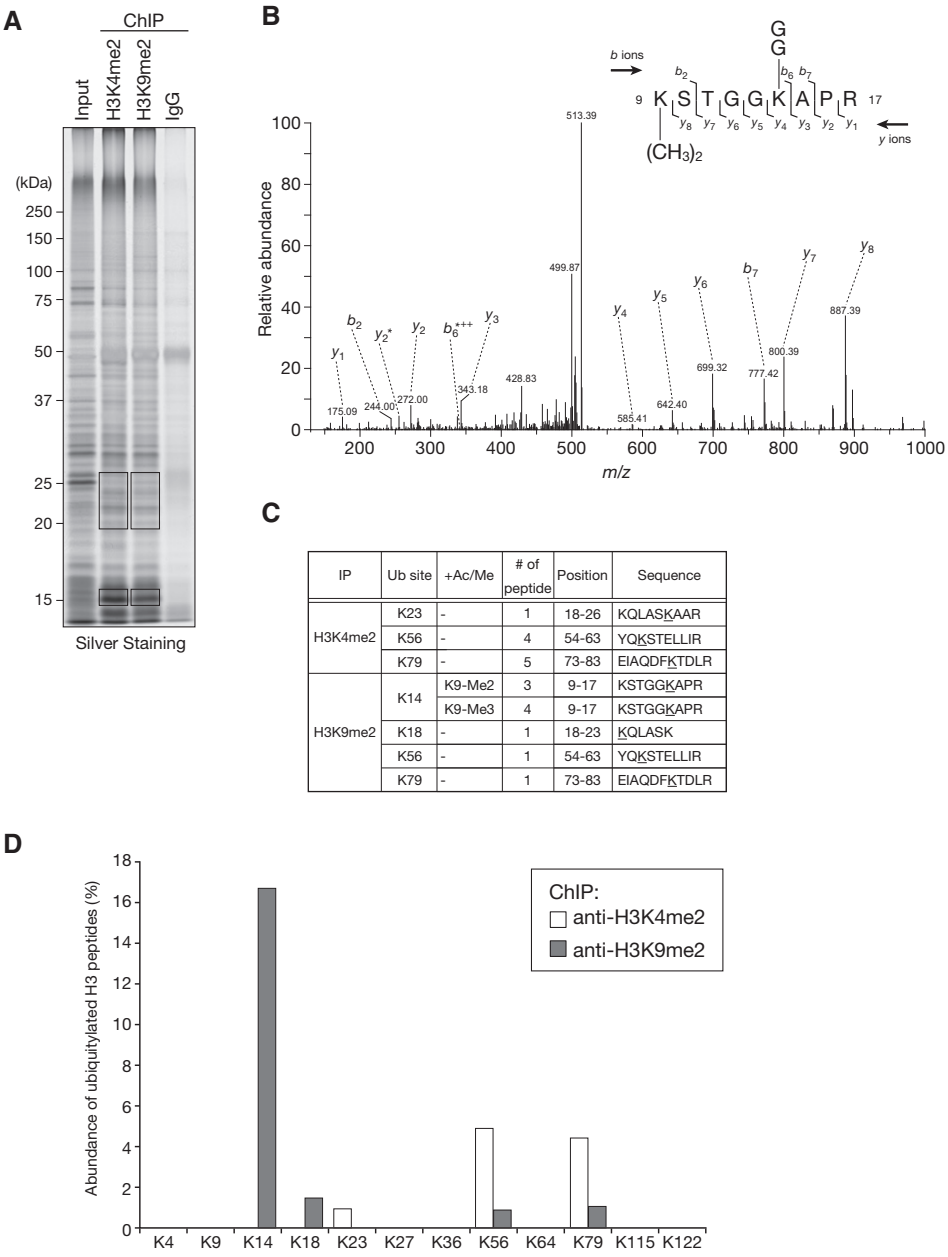

IP	Ub site	+Ac/Me	# of peptide	Position	Sequence
H3K4me2	K23	-	1	18-26	KQLASKAAR
	K56	-	4	54-63	YQKSTELLIR
	K79	-	5	73-83	EIAQDFKTDLR
H3K9me2	K14	K9-Me2	3	9-17	KSTGGKAPR
		K9-Me3	4	9-17	KSTGGKAPR
	K18	-	1	18-23	KQLASK
	K56	-	1	54-63	YQKSTELLIR
	K79	-	1	73-83	EIAQDFKTDLR

Figure 3. H3K14 ubiquitylation is associated with H3K9me-enriched chromatin.

A Chromatin precipitated with anti-H3K4me2 or anti-H3K9me2 antibodies was analyzed by SDS–PAGE and silver staining. The input sample and mock precipitation using total mouse IgG are also shown. The gel slices indicated by boxes were excised and subjected to LC-MS/MS analysis.

B MS/MS spectrum of the histone H3 peptide corresponding to residues 9–17. The observed *y* and *b* ions and fragment map are shown.

C Summary of the ubiquitylated peptides identified by LC-MS/MS.

D Relative abundance of ubiquitylated lysine residues in chromatin-associated histone H3 fractions. Chromatin precipitated with anti-H3K4me2 or anti-H3K9me2 antibodies was subjected to LC-MS/MS analysis, and the abundance of ubiquitylated lysine residues in each fraction is shown (see also Fig EV3F). Since short peptides cleaved at unmodified lysine residues could not be efficiently detected in the LC-MS/MS analysis, these data do not accurately reflect the abundance including unmodified lysines.

(Fig EV4I and J). Thus, this effect was probably due to the reduction in H3K4me2, which was associated with active transcription of the inserted *ura4*$^+$ marker gene (Fig EV4H). Taken together, these results are consistent with previous findings [42,43] and confirmed the importance of H3K14 in H3K9me generation and heterochromatin assembly.

H3K14ub promotes H3K9me

Based on the above results, we next examined the possible connection between H3K14ub and H3K9me. To test whether H3K14ub modulates H3K9me, we performed *in vitro* histone methyltransferase (HMTase) assays using recombinant Clr4 and ubiquitylated

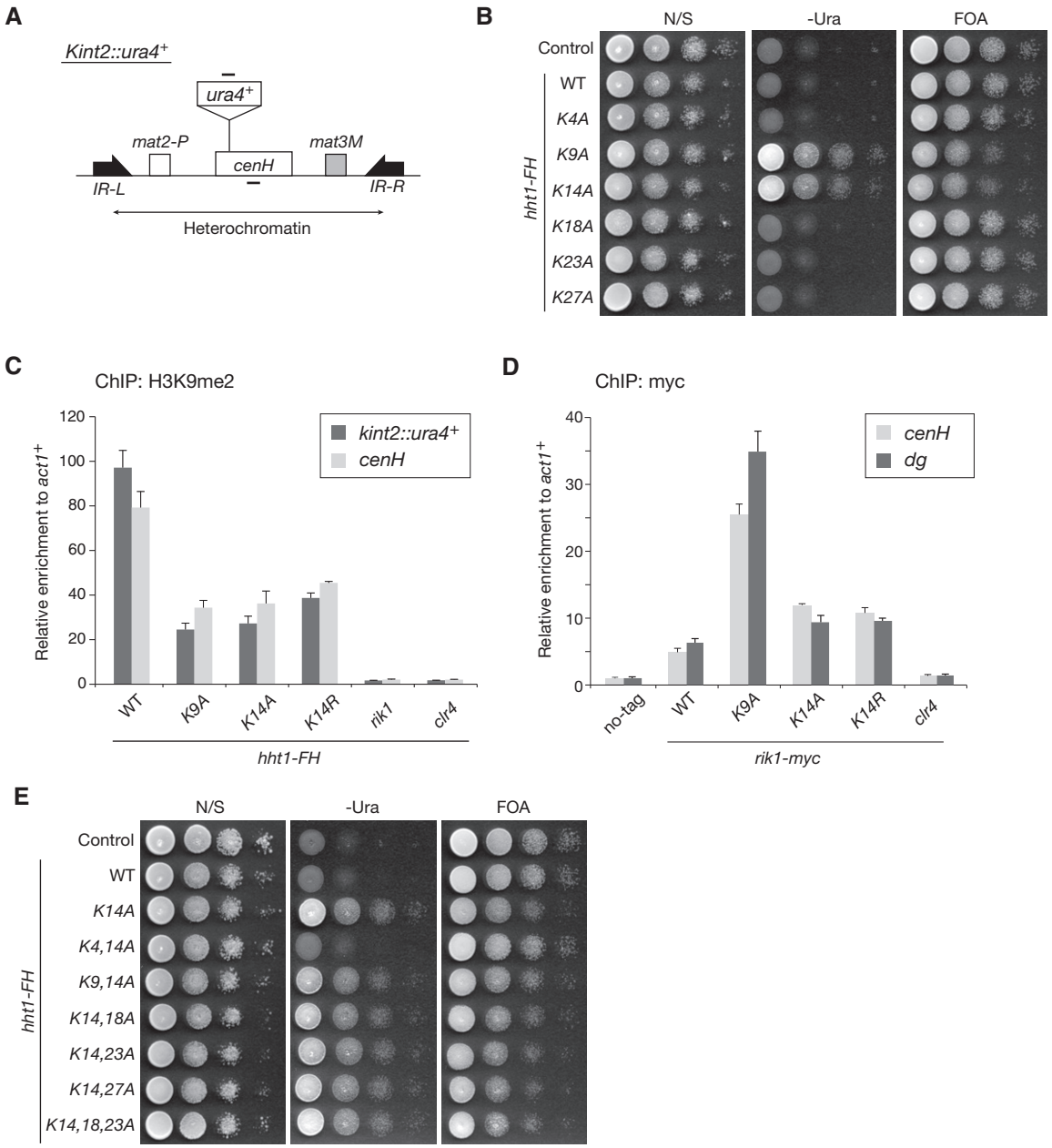

Figure 4. H3K14 is critical for heterochromatic silencing.

A Diagram of the mating-type loci in *S. pombe*. The position of the silencing reporter gene (*Kint2::ura4*$^+$) is shown. The target regions in the ChIP analysis are indicated by black bars above (*Kint2::ura4*$^+$) and below (*cenH*) in the diagram.

B Heterochromatic silencing assays of strains expressing C-terminally FLAG- and His-tagged, wild-type or mutant H3 (Hht1-FH). Silencing at the mating-type *Kint2::ura4*$^+$ was evaluated. Ten-fold serial dilutions of the indicated strains were spotted onto non-selective medium (N/S), medium lacking uracil (-Ura), and medium containing 5-FOA (5-FOA).

C ChIP analysis of H3K9me2 levels associated with the mating-type loci, relative to the control *act1*$^+$ locus. Error bars indicate standard errors from three technical replicates.

D ChIP analysis of Rik1-myc levels associated with the mating-type *cenH* and centromeric *dg* loci, relative to the control *act1*$^+$ locus. Error bars indicate standard errors from three technical replicates.

E Heterochromatic silencing assays comparing the effects of H3 lysine substitution mutants. Silencing at the mating-type *kint2::ura4*$^+$ was evaluated as in (B).

H3N-GST as a substrate (Fig 5A). H3N-GST was first subjected to an *in vitro* ubiquitylation assay using affinity-purified CLRC (as in Fig 1C). After the reaction, the resultant H3N-GST was purified and subjected to an *in vitro* HMTase assay, in which the incorporation of a radioactively labeled methyl group transferred from ^{3}H-SAM was detected by autoradiography. In the control experiments without CLRC-mediated ubiquitylation, Clr4 methylated the wild-type (WT) H3N-GST (Fig 5B, right panel, lane 2). Strikingly, even though only 10–15% of the H3N-GST was ubiquitylated by the CLRC under our assay conditions and the rest remained unmodified (Fig 5B, left

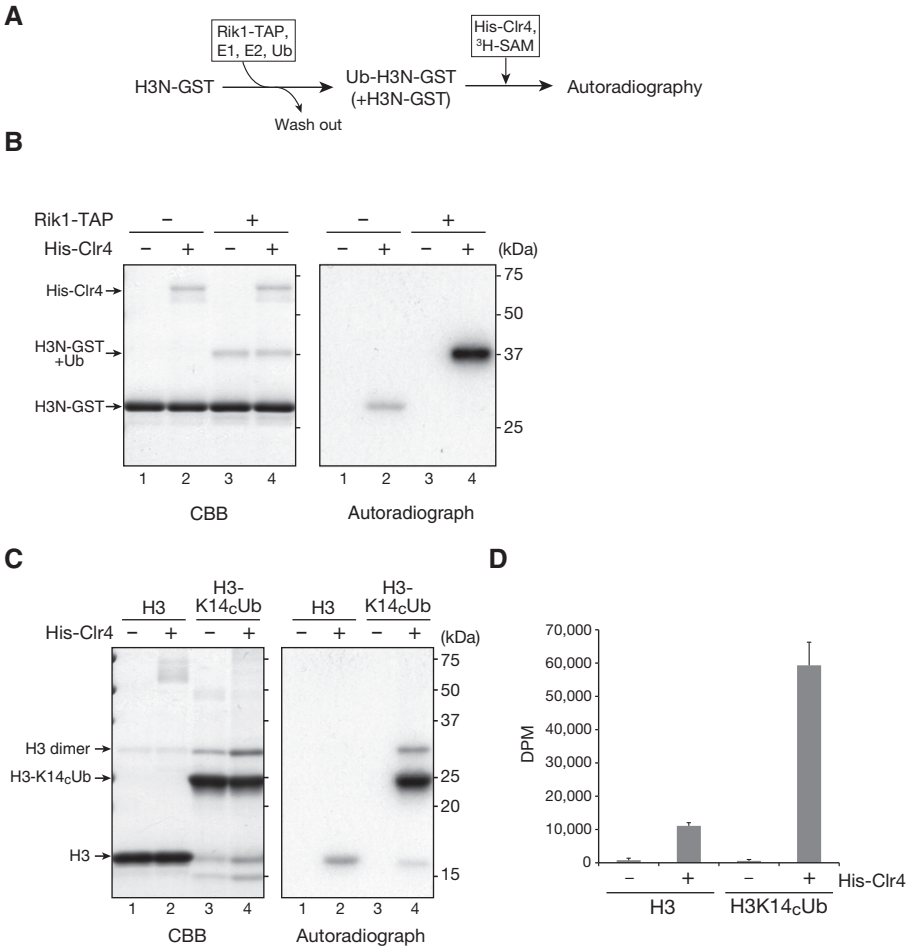

Figure 5. H3K14 ubiquitylation promotes H3K9 methylation.

A Experimental scheme.

B *In vitro* HMTase assays. Recombinant H3N-GST pre-ubiquitylated by the CLRC was purified and used in the HMTase assay with 6×His-tagged recombinant Clr4 (His-Clr4). Proteins were analyzed by SDS–PAGE and Coomassie Brilliant Blue (CBB) staining (left) and autoradiography (right).

C, D *In vitro* HMTase assay using disulfide-linked ubiquitylated histone H3. H3K14$_C$Ub and control histone H3 (H3C110A) were used as substrates in the HMTase assay and analyzed as in (B). The ^{3}H-methyl group incorporation was measured using a liquid scintillation counter (D). Error bars indicate the standard deviations calculated from three independent experiments.

panel, lanes 3 and 4), Clr4 exclusively methylated the ubiquitylated H3N-GST (Fig 5B, right panel, lane 4). In addition, the methylation of the ubiquitylated H3N-GST was much stronger than that of the control H3N-GST (Fig 5B, right panel, lanes 2 and 4), suggesting that CLRC-mediated ubiquitylation of H3 increases Clr4's HMTase activity for the H3 as a substrate.

To confirm the effect of H3K14ub on H3K9me, we prepared K14-ubiquitylated histone H3 (H3K14$_C$Ub) by disulfide cross-linking (see Materials and Methods) and used it as a substrate in the HMTase assay. Consistent with the results in Fig 5B, H3K14$_C$Ub was more efficiently methylated by Clr4 than was unmodified H3 (Fig 5C, right panel), and the incorporation of ^{3}H-labeled methyl groups was approximately six times that of the control H3 (Fig 5D). These results were consistent with those using CLRC-treated H3N-GST (Fig 5B). We also examined whether H3K9me modulates H3K14ub by using histone H3 containing a K9me3 analog (H3Kc9me3) as a substrate (see Materials and Methods). In the *in vitro* ubiquitylation assay, CLRC's ubiquitin ligase activity for histone H3 was not noticeably changed (Fig EV5, indicated by asterisks), suggesting that H3K9me does not affect K3K14ub. Taken together, these results indicated that H3K14ub promotes H3K9me and that this effect is unidirectional.

Clr4 N-terminal regions recognize ubiquitylated H3

These *in vitro* HMTase assays indicated that ubiquitylated histone H3 is recognized by Clr4. Clr4 possesses an evolutionarily conserved N-terminal chromodomain (CD) and C-terminal SET domain, and less conserved SET-associated regions (Fig 6A) [44,45]. To investigate how Clr4 recognizes ubiquitylated histone H3, we produced a series of N-terminally truncated Clr4 mutants as GST fusion proteins (Fig 6A and B) and examined their ability to recognize ubiquitylated H3 (H3K14$_C$Ub) in the HMTase assay using control histone H3 and H3K14$_C$Ub as substrates. Although GST-fused full-length (FL) Clr4

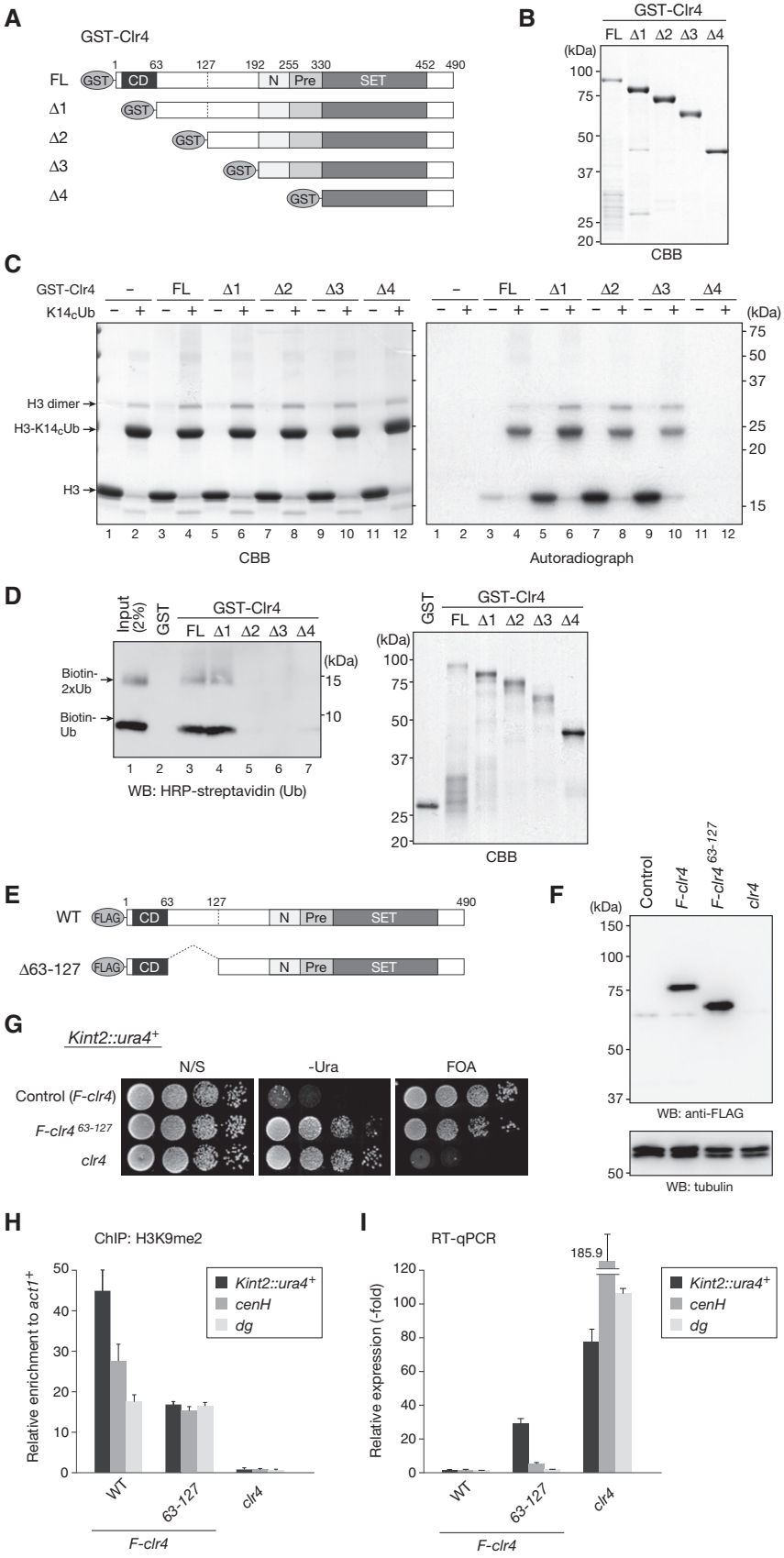

Figure 6.

Figure 6. Clr4 N-terminal regions are involved in recognizing ubiquitylated H3 and heterochromatic silencing.

A Schematic of recombinant Clr4 proteins used in the *in vitro* HMTase assay: GST-fused full-length Clr4 (FL) and truncated Clr4 proteins (Δ1-Δ4).

B Recombinant proteins used in (C) and (D) were resolved by 10% SDS–PAGE and visualized by CBB staining.

C *In vitro* HMTase assay using disulfide-linked ubiquitylated histone H3. H3K14$_C$Ub and control histone H3 (H3C110A) were used as substrates in the HMTase assay and analyzed as in Fig 5C.

D *In vitro* pull-down assays of GST-Clr4 proteins with biotinylated ubiquitin. Bound ubiquitin was analyzed by Western blotting with HRP-conjugated streptavidin (left). Precipitated GST proteins were analyzed by SDS–PAGE and CBB staining (right).

E Schematic of FLAG-tagged, wild-type, and mutant (Δ63–127) Clr4 proteins.

F Whole cell lysates prepared from control cells, cells expressing FLAG-tagged wild-type Clr4 (*F-clr4*) or mutant Clr4 (*F-clr4*$^{\Delta 63-127}$), or *clr4*Δ cells were subjected to immunoblotting using the indicated antibodies.

G Heterochromatic silencing assays of wild-type and *clr4* mutant strains. Silencing at the mating-type *Kint2::ura4*$^+$ was evaluated.

H ChIP analysis of H3K9me2 levels associated with the silencing marker gene inserted in the mating-type loci (*Kint2::ura4*$^+$) and the mating-type *cenH* and centromeric *dg* loci, relative to the control *act1*$^+$ locus. Error bars indicate standard errors from three technical replicates.

I The levels of *Kint2::ura4*$^+$, mating-type *cenH*, and centromeric *dg* transcripts were quantified by RT–qPCR and calculated as fold change to the wild-type expression. Error bars indicate standard errors from three technical replicates.

showed a specificity for H3K14$_C$Ub (Fig 6C, right panel, lanes 3 and 4), the CD-deleted Clr4 mutant (Clr4_Δ1) lost this specificity and methylated both control H3 and H3K14$_C$Ub with comparable efficiency (Fig 6C, right panel, lanes 5 and 6). Further N-terminally deleted Clr4 mutants (Clr4_Δ2 and Clr4_Δ3) appeared to show the opposite preference; the level of methylated control H3 was apparently higher than that of H3K14$_C$Ub (Fig 6C, right panel, lanes 7–10). The deletion of the N-terminal SET-associated region (Clr4_Δ4) abolished Clr4's HMTase activity (Fig 6C, right panel, lanes 11 and 12), suggesting that it has a critical role in this activity.

To confirm this result, we tested whether Clr4 binds directly to ubiquitin. We carried out GST pull-down assays using GST-fused full-length (FL)-deleted and N-terminally deleted (Δ1-Δ4) Clr4 proteins (Fig 6A and B) and biotinylated ubiquitin. GST was used as a control. Subsequent Western blots showed that the FL- and CD-deleted Δ1 proteins could bind to ubiquitin, whereas further deleted mutants (Δ2-Δ4) failed to bind ubiquitin (Fig 6D). These results suggested that the CD-adjacent N-terminal region can bind ubiquitin and contributes to the recognition of ubiquitylated H3. To further investigate the potential role of the CD-adjacent region for Clr4 function, we created fission yeast strains expressing FLAG-tagged wild-type or mutant (Δ63–127) Clr4 from its original promoter (Fig 6E and F). Notably, the deletion led to defective silencing for *Kint2::ura4*$^+$ and reduced H3K9me2 levels at *Kint2::ura4*$^+$ and *cenH* loci, although this effect was milder than that of *clr4*Δ cells (Fig 6G–I). These results suggested that the CD-adjacent N-terminal region plays an important role in Clr4's function. Interestingly, the effect of Δ63–127 deletion on *Kint2::ura4*$^+$ was comparable to that of cells expressing *hht1-K14A* (Fig EV4K), and this deletion had a negligible impact on centromeric silencing (*otr1R::ura4*$^+$) and *dg* expression (Figs 6H and I, and EV4L), implying that Clr4's enzymatic activity may be differentially regulated at each heterochromatin region.

Discussion

Here, we demonstrated that a novel modification regulates H3K9me. Our study revealed that the CLRC preferentially ubiquitylates histone H3K14 and, more importantly, that H3K14ub promotes H3K9me generation for heterochromatin assembly.

H3K14 was previously shown to play a critical role in heterochromatin assembly, and this residue is also the acetylation site associated with transcriptional activation. Either mutations in *clr3*, which encodes an H3K14-specific deacetylase, or the H3K14A substitution, which mimics the acetylated lysine, cause reduced H3K9me and defects in heterochromatic silencing [6,42,43,46,47]. These findings suggest that the deacetylation of H3K14 by Clr3 is required for H3K9's methylation by Clr4. In contrast, Clr4 efficiently methylates a K14-acetylated H3 peptide [6], and the H3K14R substitution, which mimics unacetylated lysine, also leads to a severe silencing defect [42]. These results indicated that the unacetylated state of H3K14 is not sufficient for efficient H3K9me. These apparently conflicting findings suggested that there is a gap in our understanding of how H3K14 is involved in heterochromatin assembly. Here, we demonstrated that H3K14 is modified by ubiquitylation, which promotes H3K9's methylation by Clr4. Since H3K9me did not noticeably affect the H3K14ub by CLRC (Fig EV5), H3K14ub is likely to be a prerequisite modification for H3K9me.

The chromodomain (CD) is a highly conserved protein module that is critical for targeting proteins to their action sites in chromatin. CD's best-known role is its binding to methylated histone tails. As demonstrated for the CDs in HP1 family proteins, Clr4-CD also binds K9-methylated histone H3 [15], and this activity is critical for CLRC's heterochromatic association and for stable inheritance of the H3K9me mark [15,48]. Since Clr4 and its homologs contain both CD (H3K9me reader) and SET (H3K9me writer) domains, a direct read–write mechanism has been suggested for heterochromatin spreading and epigenetic inheritance [15,48]. According to this model, Clr4 recruited by preexisting H3K9me provides new K9me on H3 in the same or neighboring nucleosomes. However, in the present study we demonstrated that Clr4's HMTase activity was enhanced by the presence of H3K14ub (Fig 5). These results suggested that the simple read–write mechanism could be revised to include the involvement of ubiquitylation. Since we also demonstrated that Clr4-CD and its neighboring regions contribute to the recognition of ubiquitylated H3 (Fig 6A–C), it is possible that Clr4-CD has multiple functions that modulate its HMTase activity for heterochromatin spreading and epigenetic inheritance [19]. In this study, we also demonstrated that Clr4 binds directly to ubiquitin via its N-terminal region (Fig 6D) and that the CD-adjacent region is critical for heterochromatic silencing (Fig 6E–I). Considering that N-terminally deleted Clr4 mutants showed a preference for unmodified H3, it is also possible that CD or a CD-adjacent region plays an inhibitory role for the SET domain's HMTase activity for unmodified H3 and that ubiquitylated H3 somehow suppresses this activity.

This notion is consistent with a very recent study on SUV39H1 [49]. Another recent study demonstrated that Clr4's catalytic activity is inhibited by an internal loop and that the automethylation of a specific lysine in the loop promotes a conformational switch that enhances Clr4's H3K9me activity [50]. Thus, the coordination of auto-regulation mechanisms may help to suppress Clr4's promiscuous activity and provide an additional system ensuring the read–write mechanism. While we clearly showed the importance of H3K14Ub and Clr4's CD-adjacent region for Clr4's function, the effect was limited to the mating-type region, and only a negligible effect was seen for centromeric heterochromatin (Fig EV4E and L). It is possible that there are additional CLRC's targets for ubiquitylation, which may redundantly promote Clr4's activity. Alternatively, Clr4's activity may also be regulated by mechanisms other than ubiquitylation [19,51].

An important issue requiring further investigation is the dynamics of H3K14ub. Since H3K9me is coupled with the deposition of newly synthesized histones after DNA synthesis, H3K14's ubiquitylation and de-ubiquitylation may be cell-cycle-dependent, as well. Although 20 de-ubiquitylating enzymes are expressed in *S. pombe*, a specific de-ubiquitylating enzyme(s) that targets heterochromatin have not been identified yet. Multiple enzymes may act cooperatively in this process. Another issue requiring clarification is the mechanism by which the CLRC is recruited to specific regions of chromatin. Although Raf1 and Raf2 have been implicated in substrate recognition [27–29], the identity of their target(s) remains unclear. Raf2 contains a domain that shows weak similarity to the RFTS of DNMT1 (a methyltransferase involved in maintaining DNA methylation) [29], and DNMT1's RFTS is known to play a role in recognizing ubiquitylated H3 [52,53]. Raf2's RFTS-like domain may also have a role in targeting ubiquitylated H3. Alternatively, it is possible that Raf2's RFTS has a distinct role in CLRC function, unrelated to H3 ubiquitylation [29].

In *Neurospora crassa*, the H3K9 methyltransferase Dim-5 forms a complex with Cul4 and DDB1 called the DCDC, which is required for Dim-5-mediated H3K9me [54]. In human cells, CUL4 is associated with SUV39H1 [55], and depleting CUL4 or DDB1 impairs H3K9me [56]. In addition, CUL4-DDB1 has been shown to have ubiquitin ligase activity for H3 [57], and proteomic surveys using human cells revealed that H3K14 is ubiquitylated *in vivo* [40]. It is therefore likely that H3 ubiquitylation mediated by CUL4-DDB1 plays an important role in the methylation of H3K9 in other systems. The ubiquitin ligase activity of CUL4-DDB1 promotes H3 polyubiquitylation [58], which appears to be distinct from the CLRC-mediated ubiquitylation we observed. In our *in vitro* ubiquitylation assay, the major products detected were mono- and di-ubiquitylated species, and other multiply ubiquitylated species were not clearly detected (Fig 1C). However, it is possible that the combination of appropriate DCAF(s) (DDB1 and CUL4-associated factors) modulates CUL4-DDB1's activity and provides substrate specificity [59].

Cross-talk between histone ubiquitylation and methylation is well known to occur for H2B mono-ubiquitylation and H3K4 methylation [36]. It was also recently reported that histone H2A's mono-ubiquitylation promotes H3K27's methylation [37] and that H3's ubiquitylation plays a role in the maintenance of DNA methylation [52,53]. Although it has been suggested that ubiquitin functions as an adaptor to recruit other modifying enzymes, the underlying molecular mechanisms of this action are not fully understood. Further analysis of the functional interactions between H3K14ub and H3K9me will provide additional insight into the cross-talk between histone ubiquitylation and methylation and the role it plays in chromatin assembly.

Materials and Methods

Strains and plasmids

The *S. pombe* strains used in this study are described in Appendix Table S2. The media and genetic methods used in the study were described previously [60]. The *cul4-1* strain was generated by inserting the hygromycin-resistant gene into the 3′ untranslated region of the *cul4* gene. For the deletion or epitope tagging of target genes, the PCR-based module method was used [61]. To produce H3N-GST fusion proteins in *E. coli*, the portion of the histone H3 coding sequence corresponding to amino acids 1–36 was amplified by PCR and cloned into the pCold IV vector (Takara), followed by downstream insertion of the GST coding sequence. Site-directed mutagenesis was used to introduce each of the amino acid substitutions.

Antibodies

The following antibodies were used in this study: anti-biotin (7075; Cell Signaling Technology), anti-histone H2A (ab13923; Abcam), anti-histone H2B (63-125; BioAcademia), anti-histone H3 (rat, 1G1; kindly provided by H. Kimura [62]), anti-histone H4 (mouse, 9C5; kindly provided by H. Kimura), anti-H3K9me2 (mouse; kindly provided by T. Urano [63]: MABI0307, MAB Institute, Inc.), anti-H3K4me2 (MABI0303; MAB Institute, Inc.), horseradish peroxidase (HRP)-conjugated anti-FLAG M2 (A8592; Sigma), anti-tubulin (T5168; Sigma), HRP-conjugated streptavidin (21130; Thermo), HRP-conjugated anti-mouse IgG (112–035-072; Jackson ImmunoResearch), HRP-conjugated anti-rabbit IgG (A6667; Sigma), and HRP-conjugated anti-rat IgG (NA935; GE Healthcare). Anti-GST rabbit polyclonal antibodies were prepared and affinity-purified using recombinant GST protein.

Tandem affinity purification

Rik1-TAP purification was performed as described previously [64], with some modifications. Exponentially growing cells (6.4×10^{11} cells) were harvested by centrifugation, washed once in phosphate-buffered saline (PBS), and transferred to 50-ml tubes (approximately 8 g per tube, 16 tubes). The pelleted cells were frozen with liquid nitrogen and stored at −80°C before further purification. All subsequent steps were performed at 4°C. The frozen cells in each tube were resuspended in 10 ml of TAP lysis buffer (50 mM HEPES [pH 7.5], 300 mM potassium acetate, 20 mM β-glycerophosphate, 5 mM magnesium acetate, 1 mM EGTA, 1 mM EDTA, 0.1% Nonidet P-40 [NP-40], 1 mM dithiothreitol [DDT], 1 mM phenylmethylsulfonyl fluoride [PMSF]), supplemented with protease inhibitor cocktail (Complete; Roche), and lysed by glass-bead breakage in a Multi Beads Shocker (Yasui Kikai). The crude lysate in each tube was diluted with 15 ml of TAP lysis buffer and incubated with gentle agitation on a disk rotator for 30 min. The lysates were then centrifuged at 12,000 ×*g* for 20 min, and the cleared lysates

(approximately 20 mg/ml protein) were pooled and divided into 12 aliquots. Each aliquot was further purified as previously described [64]. For LC-MS/MS analysis, the eluted proteins were precipitated by adding 2 volumes of ethanol and resolved by SDS–PAGE. For the ubiquitylation assay, the eluted proteins were dialyzed against Ubc buffer (50 mM HEPES [pH 7.3], 150 mM NaCl, 10% glycerol, 1 mM DTT) and concentrated using Amicon Ultra (Merck Millipore). The eluate derived from 6.4×10^{11} cells was concentrated to approximately 150 μl.

Recombinant protein production

The cDNAs of *S. pombe* histones (H2A [*hta1*$^+$], H2B [*htb1*$^+$], H3 [*hht1*$^+$], and H4 [*hhf1*$^+$]) and human H3 were PCR-amplified and cloned into the pET-3a vector (Merck Millipore). Recombinant histones were expressed in BL21 (DE3) *E. coli* and purified as described previously [65]. To generate the H3K9me3 analog, human histone H3.2 containing K9C and C110A substitutions was expressed and purified as for the other histones. The purified H3 K9C/C110A protein was subjected to alkylation as previously described [66]. Recombinant GST-fused and 6×His-tagged proteins were expressed in BL21 (DE3) *E. coli* and purified, respectively, by Glutathione Sepharose 4B (GE Healthcare) and TALON Metal Affinity Resin (Clontech), according to the manufacturers' instructions. The eluted proteins were further purified by anion exchange chromatography (SOURCE 15Q; GE Healthcare).

In vitro ubiquitylation assays

In vitro ubiquitylation assays were performed using a Ubiquitinylation Kit (Enzo Life Sciences) according to the manufacturer's instructions with some modifications. The E1 (12.5 or 25 nM) and E2 (175 or 350 nM recombinant human UbcH5b) enzymes were mixed with 2.5–10 μl of the concentrated Rik1-TAP purified fraction and 0.5 or 1 μM substrate in 25 μl of reaction buffer, and the mixtures were incubated at 30°C for 2 h. The reactions were terminated by adding equal volumes of 2× SDS sample buffer. The proteins were resolved by SDS–PAGE and analyzed by Western blotting. Can Get Signal (Toyobo) was used to enhance the Western blotting signals.

Nucleosome reconstitution

Nucleosomes used in the *in vitro* ubiquitylation assays were prepared as described previously [67].

Nano-liquid chromatography-tandem mass spectrometry (LC-MS/MS)

The proteins in each gel slice were subjected to reduction with 10 mM dithiothreitol (DDT), at 56°C for 1 h, alkylation with 55 mM iodoacetamide at room temperature for 45 min in the dark, and digestion with 10 μg/ml modified trypsin (Promega) or 20 μg/ml ArgC (Promega) at 37°C for 16 h. The resulting peptides were extracted with 1% trifluoroacetic acid and 50% acetonitrile, dried under a vacuum, and dissolved in 2% acetonitrile and 0.1% formic acid. The peptides were then fractionated by C18 reverse-phase chromatography (ADVANCE UHPLC; AMR Inc.) and applied directly into a hybrid linear ion trap mass spectrometer (LTQ Orbitrap Velos Pro; Thermo Fisher Scientific) with Advanced Captive Spray SOURCE (AMR Inc.). The mass spectrometer was programmed to carry out 11 successive scans, with the first consisting of a full MS scan from 400–2,000 m/z by FT-ICR at a resolution of 60,000, and the second to eleventh consisting of data-dependent scans of the top ten abundant ions obtained in the first scan, by ion trap. Automatic MS/MS spectra were obtained from the highest peak in each scan by setting the relative collision energy to 35% and the exclusion time to 20 s for molecules in the same m/z value range. The molecular masses of the resulting peptides were searched against the non-redundant NCBI database using the MASCOT program. MS/MS spectra were also analyzed using MaxQuant software (version 1.5.2.8). Searches were performed using the default parameters with the following modifications: (i) The minimum peptide length was 5 amino acids, (ii) the minimum score for modified peptides was 10, and (iii) variable modification was allowed.

Immunoprecipitation of H3K4me2- or H3K9me2-associated chromatin from *S. pombe*

Exponentially growing cells (1×10^{10} cells) were treated with 5 mM N-ethylmaleimide (Nacalai Tesque) for 30 min, and then fixed with 1% formaldehyde for 30 min at 25°C. After quenching the fixation by adding 150 mM glycine, the cells were harvested and washed once with PBS and once with PBS containing 25% glycerol. The pelleted cells were frozen with liquid nitrogen and stored at −80°C until use. The pelleted cells were resuspended in 10 ml of IP buffer (50 mM HEPES [pH 7.5], 140 mM NaCl, 1 mM EDTA, 1% Triton X-100, and 0.1% Na-deoxycholate) supplemented with 1 mM PMSF and protease inhibitor cocktail (Complete; Roche), and lysed by glass-bead breakage in a Multi Beads Shocker (Yasui Kikai). The cell extract was diluted to 80 ml with IP buffer containing 1 mM PMSF and protease inhibitor cocktail, and sonicated with a Bioruptor (CosmoBio) for 240 s set at level H. After sonication, the cell extract was centrifuged at 12,000 ×g for 10 min, and the supernatants were used for immunoprecipitation. Anti-mouse IgG antibody-conjugated magnetic beads (DYNAL, 500 μl) were preincubated with 10 μg of primary antibody, anti-H3K4me2 (MABI0303; MABI) or anti-H3K9me2 (MABI0307; MABI), for 1 h at 4°C, followed by incubation with the cell extracts for 2 h at 4°C. Total mouse IgG (Millipore) was used as a control. After immunoprecipitation, the beads were washed once with IP buffer, and twice each with wash buffer A (50 mM HEPES [pH 7.5], 500 mM NaCl, 1 mM EDTA, 1% Triton X-100, and 0.1% Na-deoxycholate), wash buffer B (10 mM Tris [pH 8.0], 250 mM LiCl, 0.5% NP-40, and 0.5% Na-deoxycholate), and TES buffer (10 mM Tris [pH 7.5], 1 mM EDTA, and 250 mM NaCl). The bound proteins were eluted with 500 μl of TES buffer containing 1% SDS, precipitated by adding 2 volumes of ethanol, resolved by SDS–PAGE, and subjected to Western blotting or LC-MS/MS analysis.

Silencing assays

Silencing assays were conducted using unsaturated cultures grown in YEA medium. Serial 10-fold dilutions were spotted on plates with minimal non-selective medium containing L-glutamic acid as a nitrogen source instead of ammonium chloride (N/S), minimal

medium lacking uracil (-Ura), or minimal medium containing 5-fluoroorotic acid (5-FOA). The plates were then incubated at 30°C for 2–4 days.

Chromatin immunoprecipitation (ChIP) analysis

ChIP was performed as described previously [63]. The primers used in the ChIP analyses are described in Appendix Table S3.

Real-time quantitative reverse transcription PCR (RT–qPCR)

RT–qPCR analyses were performed as described previously [19]. The primers used in the RT–qPCR analyses are described in Appendix Table S3.

In vitro HMTase assay

HMTase assays were performed as described previously [68] with some modifications. The substrate (6.2 μM) was mixed with 0.5 μM recombinant His-Clr4 or GST-Clr4 in 25 μl of reaction buffer (50 mM Tris–HCl [pH 8.0], 10% [v/v] glycerol, 1 mM DTT, 1 mM PMSF, and 0.5 μCi of *S*-[Methyl-3H]-Adenosyl-$_L$-methionine [PerkinElmer]) and incubated at 30°C for 1 h. The reactions were terminated by adding 4× SDS sample buffer, and the proteins were resolved by SDS–PAGE and visualized by autoradiography. To quantify the level of methylated histones, the reactions were quenched with cold 5% (v/v) trichloroacetic acid and subjected to filter-binding assays followed by scintillation counting.

Synthesis of K14$_C$-ubiquitylated histone H3

Disulfide-linked ubiquitylated histone H3 was synthesized as described previously [69]. Human recombinant histone H3.2 proteins containing K14C and C110A substitutions were expressed in BL21 (DE3) *E. coli* and purified as described previously [67]. Purified H3.2 proteins were reacted with 2,2′-dithiobis(5-nitropyridine) (DTNP) and dialyzed against sterile water. The ubiquitin–cysteamine fusion protein was produced as described previously [66] with some modifications. The DNA fragment encoding human ubiquitin was inserted into the pTXB1 vector, and the C-terminally Intein-CBD (chitin-binding domain)-fused ubiquitin produced in BL21 (DE3) *E. coli* was purified with a chitin column (New England Biolabs). Ubiquitin was cleaved from the Intein-CBD portion by incubating with cysteamine-dihydrochloride (Sigma-Aldrich). The eluted ubiquitin with a C-terminal aminoethanethiol linker was further purified by gel filtration chromatography (HiLoad 26/60 Superdex 75 pg; GE Healthcare), dialyzed against sterile water, and lyophilized. The purified DTNP-reacted histone H3 and ubiquitin–cysteamine were allowed to react at pH 6.9 to form the disulfide-linked ubiquitylated histone H3 (H3K14$_C$Ub). H3K14$_C$Ub was purified with a MonoS column (GE Healthcare) and used as a substrate in the *in vitro* histone methyltransferase (HMTase) assay.

GST pull-down assays

GST-fused, full-length, and truncated Clr4 proteins were incubated with biotinylated ubiquitin (BML-UW8705; Enzo Life Sciences) in binding buffer (25 mM Tris–HCl [pH 8.0], 100 mM NaCl, 10% glycerol, 0.2% NP-40) at 25°C for 2 h. GST fusion proteins and associated proteins were pulled down by adding 5 μl of Glutathione Magnetic Beads (88821; Thermo Scientific). After beads were washed with washing buffer (125 mM Tris–HCl [pH 8.0], 150 mM NaCl, 0.01% Tween 20), bound proteins were eluted by boiling with 2× SDS sample buffer. The eluted proteins were resolved by 15% SDS–PAGE, and the pulled-down biotinylated ubiquitin was detected by Western blotting using HRP-conjugated streptavidin (21130; Thermo Scientific).

Expanded View for this article is available online.

Acknowledgements
We thank H. Kimura, T. Urano, and H. Kato for the antibodies and R. Allshire for strains. We also thank E. Suzuki, T. Kawaguchi, A. Hachisuka, and R. Nakamura for technical help, and Y. Nishiyama, A. Hayashi, K. Hiragami-Hamada, K. Kataoka, and K. Tanaka for critical reading of the manuscript. The authors have no financial interests related to this work. This research was supported by KAKENHI (JP23114005, JP26291072, JP17H03713, and JP18H05532 to J.N., and JP18H05534 to H.K.), the Mochida Memorial Foundation for Medical and Pharmaceutical Research (to J.N.), the Uehara Memorial Foundation (to J.N.), the Takeda Science Foundation (to J.N.), and the Swedish Cancer Society and the Swedish Research Council (to K.E).

Author contributions
EO and JN designed the research. EO, RN, YY, MT, GN, and AS performed the experiments. SM, HK, and HT contributed to generate histone-related reagents. KE gave valuable advice and helped with supervision of EO. EO and JN wrote the manuscript, and all authors commented and edited the manuscript.

Conflict of interest
The authors declare that they have no conflict of interest.

References

1. Richards EJ, Elgin SC (2002) Epigenetic codes for heterochromatin formation and silencing: rounding up the usual suspects. *Cell* 108: 489 – 500
2. Grewal SI, Moazed D (2003) Heterochromatin and epigenetic control of gene expression. *Science* 301: 798 – 802
3. Grewal SI, Jia S (2007) Heterochromatin revisited. *Nat Rev Genet* 8: 35 – 46
4. Bannister AJ, Zegerman P, Partridge JF, Miska EA, Thomas JO, Allshire RC, Kouzarides T (2001) Selective recognition of methylated lysine 9 on histone H3 by the HP1 chromo domain. *Nature* 410: 120 – 124
5. Lachner M, O'Carroll D, Rea S, Mechtler K, Jenuwein T (2001) Methylation of histone H3 lysine 9 creates a binding site for HP1 proteins. *Nature* 410: 116 – 120
6. Nakayama J, Rice JC, Strahl BD, Allis CD, Grewal SI (2001) Role of histone H3 lysine 9 methylation in epigenetic control of heterochromatin assembly. *Science* 292: 110 – 113
7. Nakayama J, Klar AJ, Grewal SI (2000) A chromodomain protein, Swi6, performs imprinting functions in fission yeast during mitosis and meiosis. *Cell* 101: 307 – 317
8. Hall IM, Shankaranarayana GD, Noma K, Ayoub N, Cohen A, Grewal SI (2002) Establishment and maintenance of a heterochromatin domain. *Science* 297: 2232 – 2237

9. Allshire RC, Nimmo ER, Ekwall K, Javerzat JP, Cranston G (1995) Mutations derepressing silent centromeric domains in fission yeast disrupt chromosome segregation. *Genes Dev* 9: 218 – 233
10. Ivanova AV, Bonaduce MJ, Ivanov SV, Klar AJ (1998) The chromo and SET domains of the Clr4 protein are essential for silencing in fission yeast. *Nat Genet* 19: 192 – 195
11. Sadaie M, Iida T, Urano T, Nakayama J (2004) A chromodomain protein, Chp1, is required for the establishment of heterochromatin in fission yeast. *EMBO J* 23: 3825 – 3835
12. Sadaie M, Kawaguchi R, Ohtani Y, Arisaka F, Tanaka K, Shirahige K, Nakayama J (2008) Balance between distinct HP1 family proteins controls heterochromatin assembly in fission yeast. *Mol Cell Biol* 28: 6973 – 6988
13. Motamedi MR, Hong EJ, Li X, Gerber S, Denison C, Gygi S, Moazed D (2008) HP1 proteins form distinct complexes and mediate heterochromatic gene silencing by nonoverlapping mechanisms. *Mol Cell* 32: 778 – 790
14. Fischer T, Cui B, Dhakshnamoorthy J, Zhou M, Rubin C, Zofall M, Veenstra TD, Grewal SI (2009) Diverse roles of HP1 proteins in heterochromatin assembly and functions in fission yeast. *Proc Natl Acad Sci USA* 106: 8998 – 9003
15. Zhang K, Mosch K, Fischle W, Grewal SI (2008) Roles of the Clr4 methyltransferase complex in nucleation, spreading and maintenance of heterochromatin. *Nat Struct Mol Biol* 15: 381 – 388
16. Moazed D (2009) Small RNAs in transcriptional gene silencing and genome defence. *Nature* 457: 413 – 420
17. Goto DB, Nakayama J (2012) RNA and epigenetic silencing: insight from fission yeast. *Dev Growth Differ* 54: 129 – 141
18. Castel SE, Martienssen RA (2013) RNA interference in the nucleus: roles for small RNAs in transcription, epigenetics and beyond. *Nat Rev Genet* 14: 100 – 112
19. Ishida M, Shimojo H, Hayashi A, Kawaguchi R, Ohtani Y, Uegaki K, Nishimura Y, Nakayama J (2012) Intrinsic nucleic acid-binding activity of Chp1 chromodomain is required for heterochromatic gene silencing. *Mol Cell* 47: 228 – 241
20. Jia S, Noma K, Grewal SI (2004) RNAi-independent heterochromatin nucleation by the stress-activated ATF/CREB family proteins. *Science* 304: 1971 – 1976
21. Kanoh J, Sadaie M, Urano T, Ishikawa F (2005) Telomere binding protein Taz1 establishes Swi6 heterochromatin independently of RNAi at telomeres. *Curr Biol* 15: 1808 – 1819
22. Horn PJ, Bastie JN, Peterson CL (2005) A Rik1-associated, cullin-dependent E3 ubiquitin ligase is essential for heterochromatin formation. *Genes Dev* 19: 1705 – 1714
23. Li F, Goto DB, Zaratiegui M, Tang X, Martienssen R, Cande WZ (2005) Two novel proteins, dos1 and dos2, interact with rik1 to regulate heterochromatic RNA interference and histone modification. *Curr Biol* 15: 1448 – 1457
24. Hong EJ, Villen J, Gerace EL, Gygi SP, Moazed D (2005) A cullin E3 ubiquitin ligase complex associates with Rik1 and the Clr4 histone H3-K9 methyltransferase and is required for RNAi-mediated heterochromatin formation. *RNA Biol* 2: 106 – 111
25. Jia S, Kobayashi R, Grewal SI (2005) Ubiquitin ligase component Cul4 associates with Clr4 histone methyltransferase to assemble heterochromatin. *Nat Cell Biol* 7: 1007 – 1013
26. Thon G, Hansen KR, Altes SP, Sidhu D, Singh G, Verhein-Hansen J, Bonaduce MJ, Klar AJ (2005) The Clr7 and Clr8 directionality factors and the Pcu4 cullin mediate heterochromatin formation in the fission yeast *Schizosaccharomyces pombe*. *Genetics* 171: 1583 – 1595
27. Buscaino A, White SA, Houston DR, Lejeune E, Simmer F, de Lima Alves F, Diyora PT, Urano T, Bayne EH, Rappsilber J *et al* (2012) Raf1 Is a DCAF for the Rik1 DDB1-like protein and has separable roles in siRNA generation and chromatin modification. *PLoS Genet* 8: e1002499
28. Kuscu C, Zaratiegui M, Kim HS, Wah DA, Martienssen RA, Schalch T, Joshua-Tor L (2014) CRL4-like Clr4 complex in *Schizosaccharomyces pombe* depends on an exposed surface of Dos1 for heterochromatin silencing. *Proc Natl Acad Sci USA* 111: 1795 – 1800
29. White SA, Buscaino A, Sanchez-Pulido L, Ponting CP, Nowicki MW, Allshire RC (2014) The RFTS domain of Raf2 is required for Cul4 interaction and heterochromatin integrity in fission yeast. *PLoS ONE* 9: e104161
30. Motamedi MR, Verdel A, Colmenares SU, Gerber SA, Gygi SP, Moazed D (2004) Two RNAi complexes, RITS and RDRC, physically interact and localize to noncoding centromeric RNAs. *Cell* 119: 789 – 802
31. Bayne EH, White SA, Kagansky A, Bijos DA, Sanchez-Pulido L, Hoe KL, Kim DU, Park HO, Ponting CP, Rappsilber J *et al* (2010) Stc1: a critical link between RNAi and chromatin modification required for heterochromatin integrity. *Cell* 140: 666 – 677
32. He C, Pillai SS, Taglini F, Li F, Ruan K, Zhang J, Wu J, Shi Y, Bayne EH (2013) Structural analysis of Stc1 provides insights into the coupling of RNAi and chromatin modification. *Proc Natl Acad Sci USA* 110: E1879 – E1888
33. Gerace EL, Halic M, Moazed D (2010) The methyltransferase activity of Clr4Suv39h triggers RNAi independently of histone H3K9 methylation. *Mol Cell* 39: 360 – 372
34. Pan ZQ, Kentsis A, Dias DC, Yamoah K, Wu K (2004) Nedd8 on cullin: building an expressway to protein destruction. *Oncogene* 23: 1985 – 1997
35. Li F, Martienssen R, Cande WZ (2011) Coordination of DNA replication and histone modification by the Rik1-Dos2 complex. *Nature* 475: 244 – 248
36. Chandrasekharan MB, Huang F, Sun ZW (2010) Histone H2B ubiquitination and beyond: regulation of nucleosome stability, chromatin dynamics and the trans-histone H3 methylation. *Epigenetics* 5: 460 – 468
37. Kalb R, Latwiel S, Baymaz HI, Jansen PW, Muller CW, Vermeulen M, Muller J (2014) Histone H2A monoubiquitination promotes histone H3 methylation in Polycomb repression. *Nat Struct Mol Biol* 21: 569 – 571
38. Jensen JP, Bates PW, Yang M, Vierstra RD, Weissman AM (1995) Identification of a family of closely related human ubiquitin conjugating enzymes. *J Biol Chem* 270: 30408 – 30414
39. Tan P, Fuchs SY, Chen A, Wu K, Gomez C, Ronai Z, Pan ZQ (1999) Recruitment of a ROC1-CUL1 ubiquitin ligase by Skp1 and HOS to catalyze the ubiquitination of I kappa B alpha. *Mol Cell* 3: 527 – 533
40. Kim W, Bennett EJ, Huttlin EL, Guo A, Li J, Possemato A, Sowa ME, Rad R, Rush J, Comb MJ *et al* (2011) Systematic and quantitative assessment of the ubiquitin-modified proteome. *Mol Cell* 44: 325 – 340
41. Cam HP, Sugiyama T, Chen ES, Chen X, FitzGerald PC, Grewal SI (2005) Comprehensive analysis of heterochromatin- and RNAi-mediated epigenetic control of the fission yeast genome. *Nat Genet* 37: 809 – 819
42. Mellone BG, Ball L, Suka N, Grunstein MR, Partridge JF, Allshire RC (2003) Centromere silencing and function in fission yeast is governed by the amino terminus of histone H3. *Curr Biol* 13: 1748 – 1757
43. Alper BJ, Job G, Yadav RK, Shanker S, Lowe BR, Partridge JF (2013) Sir2 is required for Clr4 to initiate centromeric heterochromatin assembly in fission yeast. *EMBO J* 32: 2321 – 2335
44. Aagaard L, Laible G, Selenko P, Schmid M, Dorn R, Schotta G, Kuhfittig S, Wolf A, Lebersorger A, Singh PB *et al* (1999) Functional mammalian

homologues of the *Drosophila* PEV-modifier Su(var)3-9 encode centromere-associated proteins which complex with the heterochromatin component M31. *EMBO J* 18: 1923 – 1938

45. Rea S, Eisenhaber F, O'Carroll D, Strahl BD, Sun ZW, Schmid M, Opravil S, Mechtler K, Ponting CP, Allis CD *et al* (2000) Regulation of chromatin structure by site-specific histone H3 methyltransferases. *Nature* 406: 593 – 599
46. Bjerling P, Silverstein RA, Thon G, Caudy A, Grewal S, Ekwall K (2002) Functional divergence between histone deacetylases in fission yeast by distinct cellular localization and *in vivo* specificity. *Mol Cell Biol* 22: 2170 – 2181
47. Wiren M, Silverstein RA, Sinha I, Walfridsson J, Lee HM, Laurenson P, Pillus L, Robyr D, Grunstein M, Ekwall K (2005) Genomewide analysis of nucleosome density histone acetylation and HDAC function in fission yeast. *EMBO J* 24: 2906 – 2918
48. Ragunathan K, Jih G, Moazed D (2015) Epigenetics. Epigenetic inheritance uncoupled from sequence-specific recruitment. *Science* 348: 1258699
49. Muller MM, Fierz B, Bittova L, Liszczak G, Muir TW (2016) A two-state activation mechanism controls the histone methyltransferase Suv39h1. *Nat Chem Biol* 12: 188 – 193
50. Iglesias N, Currie MA, Jih G, Paulo JA, Siuti N, Kalocsay M, Gygi SP, Moazed D (2018) Automethylation-induced conformational switch in Clr4 (Suv39h) maintains epigenetic stability. *Nature* 560: 504 – 508
51. Akoury E, Ma G, Demolin S, Bronner C, Zocco M, Cirilo A, Ivic N, Halic M (2019) Disordered region of H3K9 methyltransferase Clr4 binds the nucleosome and contributes to its activity. *Nucleic Acids Res* 47: 6726 – 6736
52. Nishiyama A, Yamaguchi L, Sharif J, Johmura Y, Kawamura T, Nakanishi K, Shimamura S, Arita K, Kodama T, Ishikawa F *et al* (2013) Uhrf1-dependent H3K23 ubiquitylation couples maintenance DNA methylation and replication. *Nature* 502: 249 – 253
53. Ishiyama S, Nishiyama A, Saeki Y, Moritsugu K, Morimoto D, Yamaguchi L, Arai N, Matsumura R, Kawakami T, Mishima Y *et al* (2017) Structure of the Dnmt1 reader module complexed with a unique two-mono-ubiquitin mark on histone H3 reveals the basis for DNA methylation maintenance. *Mol Cell* 68: 350 – 360 e7
54. Lewis ZA, Adhvaryu KK, Honda S, Shiver AL, Knip M, Sack R, Selker EU (2010) DNA methylation and normal chromosome behavior in Neurospora depend on five components of a histone methyltransferase complex, DCDC. *PLoS Genet* 6: e1001196
55. Yang Y, Liu R, Qiu R, Zheng Y, Huang W, Hu H, Ji Q, He H, Shang Y, Gong Y *et al* (2015) CRL4B promotes tumorigenesis by coordinating with SUV39H1/HP1/DNMT3A in DNA methylation-based epigenetic silencing. *Oncogene* 34: 104 – 118
56. Higa LA, Wu M, Ye T, Kobayashi R, Sun H, Zhang H (2006) CUL4-DDB1 ubiquitin ligase interacts with multiple WD40-repeat proteins and regulates histone methylation. *Nat Cell Biol* 8: 1277 – 1283
57. Wang H, Zhai L, Xu J, Joo HY, Jackson S, Erdjument-Bromage H, Tempst P, Xiong Y, Zhang Y (2006) Histone H3 and H4 ubiquitylation by the CUL4-DDB-ROC1 ubiquitin ligase facilitates cellular response to DNA damage. *Mol Cell* 22: 383 – 394
58. Han J, Zhang H, Zhang H, Wang Z, Zhou H, Zhang Z (2013) A Cul4 E3 ubiquitin ligase regulates histone hand-off during nucleosome assembly. *Cell* 155: 817 – 829
59. Angers S, Li T, Yi X, MacCoss MJ, Moon RT, Zheng N (2006) Molecular architecture and assembly of the DDB1-CUL4A ubiquitin ligase machinery. *Nature* 443: 590 – 593
60. Moreno S, Klar A, Nurse P (1991) Molecular genetic analysis of fission yeast *Schizosaccharomyces pombe*. *Methods Enzymol* 194: 795 – 823
61. Bahler J, Wu JQ, Longtine MS, Shah NG, McKenzie A III, Steever AB, Wach A, Philippsen P, Pringle JR (1998) Heterologous modules for efficient and versatile PCR-based gene targeting in *Schizosaccharomyces pombe*. *Yeast* 14: 943 – 951
62. Nozawa RS, Nagao K, Masuda HT, Iwasaki O, Hirota T, Nozaki N, Kimura H, Obuse C (2010) Human POGZ modulates dissociation of HP1alpha from mitotic chromosome arms through Aurora B activation. *Nat Cell Biol* 12: 719 – 727
63. Oya E, Kato H, Chikashige Y, Tsutsumi C, Hiraoka Y, Murakami Y (2013) Mediator directs co-transcriptional heterochromatin assembly by RNA interference-dependent and -independent pathways. *PLoS Genet* 9: e1003677
64. Kitano E, Hayashi A, Kanai D, Shinmyozu K, Nakayama J (2011) Roles of fission yeast Grc3 protein in ribosomal RNA processing and heterochromatic gene silencing. *J Biol Chem* 286: 15391 – 15402
65. Luger K, Rechsteiner TJ, Richmond TJ (1999) Preparation of nucleosome core particle from recombinant histones. *Methods Enzymol* 304: 3 – 19
66. Simon MD, Chu F, Racki LR, de la Cruz CC, Burlingame AL, Panning B, Narlikar GJ, Shokat KM (2007) The site-specific installation of methyllysine analogs into recombinant histones. *Cell* 128: 1003 – 1012
67. Tachiwana H, Kagawa W, Osakabe A, Kawaguchi K, Shiga T, Hayashi-Takanaka Y, Kimura H, Kurumizaka H (2010) Structural basis of instability of the nucleosome containing a testis-specific histone variant, human H3T. *Proc Natl Acad Sci USA* 107: 10454 – 10459
68. Sadaie M, Shinmyozu K, Nakayama J (2008) A conserved SET domain methyltransferase, Set11, modifies ribosomal protein Rpl12 in fission yeast. *J Biol Chem* 283: 7185 – 7195
69. Chatterjee C, McGinty RK, Fierz B, Muir TW (2010) Disulfide-directed histone ubiquitylation reveals plasticity in hDot1L activation. *Nat Chem Biol* 6: 267 – 269